Coherent Synchrotron Radiation measurements in the THz region at the CLS Far Infrared Beamline

Timothy E. May[a], John C. Bergstrom[a], Les O. Dallin[a], and Dominique R. T. Appadoo[b]
[a]Canadian Light Source, Inc., Saskatoon, SK S7N 0X4 Canada
[b]Australian Synchrotron Company, Ltd., Clayton, VIC 3168 Australia

***Abstract*—Synchrotron radiation (SR) in the far infrared region is used for high spectral resolution experiments at the Canadian Light Source (CLS). Although SR photon flux can exceed that of thermal sources at long wavelengths, a further increase in flux is obtained by shortening electron bunch lengths to the order of far infrared wavelengths. When shortened, the electron bunch photon output is boosted by coherent summation of the synchrotron radiation (CSR). Accelerator parameters were adjusted for short bunch lengths and CSR in burst mode at the Far Infrared beamline was observed. Preliminary results are discussed in the 5 to 40 cm^{-1} region (0.15 to 1.2 THz). Several unexpected features have been observed in the spectral energy curve at resolutions below 0.1 cm^{-1} (3 GHz). A theoretical model locating the spectral intensity peaks at high spectral resolution indicates that vacuum chamber geometry and side wall impedance effects may be responsible. A spectrum of nitrous oxide was obtained using the CSR.**

I. Introduction And Background

Synchrotron radiation in the infrared region is used for brightness limited experiments for either high spatial or high spectral resolution. Infrared radiation is emitted at large angles from the plane of the electron orbit, 85 mrad full angle for 10 cm^{-1} (1 mm wavelength, 0.3 THz) at 2.9 GeV and 7.1428 m bend magnet radius and is a consideration for sizing the vacuum port to extract the photon beam. Wide angle IR ports are used at 23 synchrotrons worldwide[1] with 6 more planned or being built. Interest in increasing infrared output has led to the use of edge radiation from the fringe region of the dipole bend magnet field (ANKA[2], Soleil[3], ASP[4], SRC[5]), or using coherent SR first seen in linacs and then storage rings (SURF[6], Max-Lab[7], BESSYII[8], ALS[9], NSLS[10]). Detector noise and component vibrations limit performance of the beamline so signal averaging is used to improve S/N. To increase the SR signal at long wavelengths, bunch compression to produce CSR is being explored as an alternative.

Synchrotron radiation has a characteristic opening angle that depends on beam energy and radius of orbit and flux increases linearly with the average electron current. The electrons emit without phase correlation along the bunch. Electron bunch lengths can be shortened by varying parameters of the accelerator such as the momentum compaction factor α. The nominal 35 ps bunch length (1 σ) of ~10 mm at CLS can be reduced to less than 10 ps corresponding to ~2.9 mm length. The photon output is boosted by coherent summation of the synchrotron radiation (CSR). This can extend to shorter wavelengths than the bunch[11]. CSR has been observed at the CLS Far IR beamline using a high resolution Bruker Optics IFS125HR FTIR spectrometer[12].

II. CSR Results

CSR was generated and observed for the first time at the CLS in 2007[13]. CSR was produced in the bursting mode[14] with one bunch of ~10 mA. The length of the single bunch was shortened from 35 ps to ~ 13 ps by reducing the momentum compaction α from 0.0038 to 0.0005, the onset of bursting. An increase in intensity of nearly 4 orders of magnitude was observed in the 5 – 30 cm^{-1} spectral window shown in Figure 1. The normal SR signal appears as a baseline in the figure. The region at 10 cm^{-1} is expanded to show its low intensity value ~10^{-2} au.

CSR onset occurred as bunch lengths approached 18 ps with bunch current ≥ 8 mA. The large increase in intensity relative to non-coherent output was seen with small decrements in α. The curve peaks around 10 and 18 cm^{-1} (0.30, 0.54 THz) at low resolution. The zero of the CSR is offset due to a large noise level below 5 cm^{-1} in the signal, partly from the bursting fluctuation and partly from low frequency vibrations in the beamline.

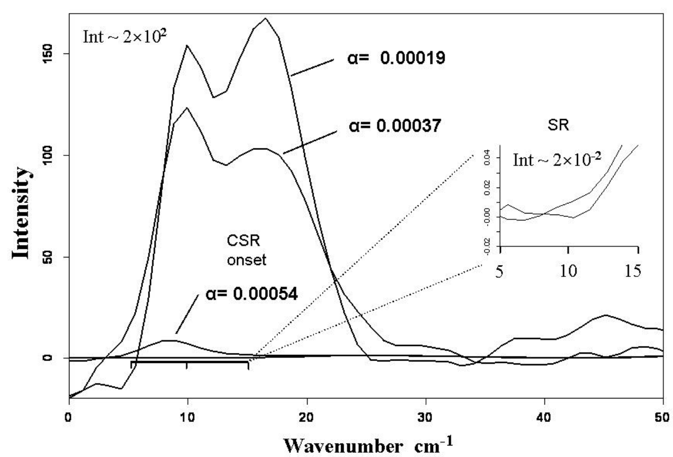

Figure 1: Signal intensity with Silicon bolometer showing increase in output as bunch length is shortened from standard 35 ps down to 13 ps times (1 σ). Inset figure shows non-CSR output, 2 cm^{-1} resolution.

Several unexpected features are observed in the spectrum at spectral resolution below 0.1 cm^{-1}. Figure 2 shows an expanded region around 7 cm^{-1} with the CSR continuous curve over a bar graph. The structure has a period of ~0.072 cm^{-1}, and in several places the peaks display a pattern of alternating high and low peak intensity. It is difficult to find a location where such a path difference can occur in our system. Interference fringes due to light reflected from the chamber outer wall was eliminated from consideration as no side wall within the field of view of the first mirror has a geometry to

978-1-4244-2120-6/08/$25.00 ©IEEE.

contribute a reflection. Fringes due to various windows in the beamline and FTIR were also eliminated. Bend magnet edge radiation could not contribute as its emission angle is too narrow and the M1 mirror is too far around the bend to intercept it. The phase of the oscillations is constant over many scans, suggesting a systematic cause. A search of possible mechanisms in the emission characteristic led to resonant modes as a possibility. A model[15] by Warnock and Morton of the radiation impedance for a toroidal chamber was applied to explain the fine structure, and indicates the outer wall contribution may be responsible. The propagating modes from the model have an alternating intensity pattern that appears to be a mechanism for the observed variation. The model calculates the impedance ratio "R/Q", where R is the amplitude of the impedance and Q is the quality factor. This gives transverse electric (TE) and magnetic (TM) mode frequencies and relative intensities for the many modes propagated with the TE modes being more intense. The overall normalization of the mode intensities is arbitrary. The model refers to a cylindrical coordinate system so these labels are not identical to the common usage for rectangular waveguides. The radial distance from the electron beam to the outer wall is the one adjustable parameter in the model used to fit the modes to the observed CSR spectrum.

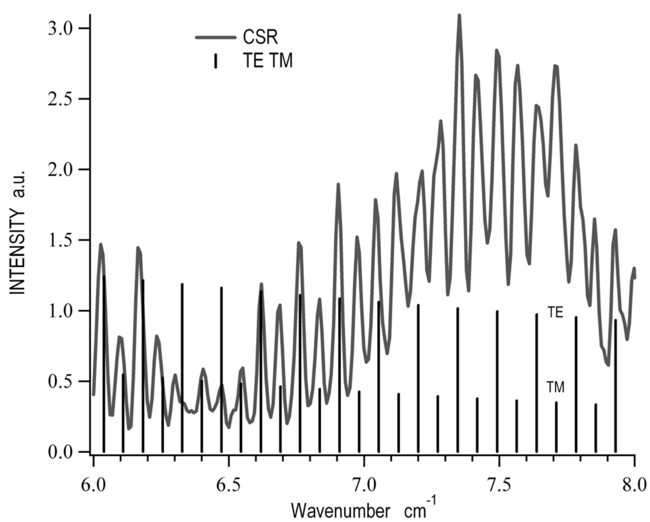

Figure 2: Overlay of the observed CSR spectrum and bars indicating TE (taller) and TM (shorter) mode locations and relative intensities (overall bar normalization is arbitrary). A single parameter, the outer wall radial distance to electron beam, fits the model to the data.

The model calculates the frequency spacing between TE (or TM) modes (difference between consecutive inverse wavelengths), and is approximated by:

$$\left(\frac{1}{\lambda}\right)_{spacing} \approx \frac{1}{2\pi R} \times \frac{3\pi}{\sqrt{8}} \times \left(\frac{R}{d}\right)^{3/2}$$

where λ is wavelength and R is electron bending radius. The variable d is distance from beam radius to outer wall, and is adjusted to line up modes with the data, over a region. This single variable lines up both the mode locations and the spacing between them, a remarkable feature of the model. The full model equations give the exact locations. Fitting the modes to peaks in the observed data gives a wall distance d = 0.2117 m over the region 6.5-8 cm^{-1}. A shift of a mode over 0.072 cm^{-1} spacing corresponds to a 1.4 mm shift in d. This distance could shift by integer amounts of 1.4 mm to overlap again, but the spacing will change. Some peaks have shoulders that displace the centers relative to the modes but on average the line up is reasonable, though it drifts off outside the region. As the modes are closely spaced, which particular mode goes with which peak cannot be specified.

The chamber is irregular compared to the cylindrical section the model assumes, with pump ports, linear sections and absorbers nearby having effects. The d value that gives the 0.144 cm^{-1} spacing between TE modes however puts the equivalent wall location at a reasonable place, along the geometric "average" distance from the beam, see Figure 3.

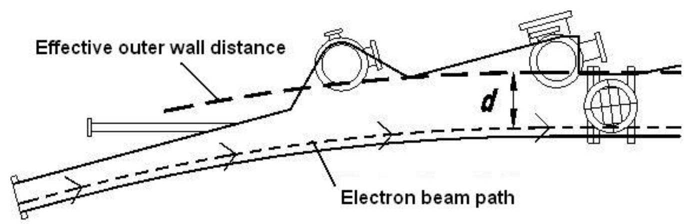

Figure 3: Top view of dipole chamber showing electron beam radius with arrows and distance d to the outer wall. M1 extraction mirror located in rectangular opening in chamber at right, outside of the magnet windings (not shown).

The phase of the fine structure persists across hours of scans so the system is stable in this respect. The modes will shift in frequency due to a change in orbit radius according to a simplified equation from the model:

$$\Delta\left(\frac{1}{\lambda}\right)_{shift} \approx \left(\frac{1}{\lambda}\right) \times \frac{3}{2} \times \left(\frac{\Delta R}{d}\right)$$

Experiments are planned to shift the beam orbit by several 100s of microns to determine whether a corresponding shift in peak locations occurs, and to use a polarizer to observe whether the modes display any polarized attributes.

The long wave cutoff of the chamber is a factor to consider for the operating range of the beamline and how it affects the mode envelope. Cutoff wavelength λ_c due to chamber geometry is approximated by

$$\lambda_c \approx 2h \times \left(\frac{h}{R}\right)^{1/2}$$

with R = 7142.8 mm and chamber height h = 32 mm giving ~4.2 mm corresponding to 2.4 cm^{-1} (0.07 THz).

The theoretical model doesn't account for any of the effects the actual beamline design has on transmission efficiency to the detector so mode intensities need modification for a more realistic match of modes to the curve appearance. Factors affecting transmission are the vertical port size, the UHV extraction window and Jacquinot stop aperture before the interferometer and gas cell and detector windows. Ratios of the SR intensity to thermal source give some measure of the transmission curve of the beamline with an exponential drop

978-1-4244-2120-6/08/$25.00 ©IEEE.

off at long wavelength a reasonable approximation[16]. The mode heights then tail off at lower frequencies to approximate the CSR curve. Some features in the intensity curve aren't explained by the model, as the modes don't return to the baseline; real impedance values don't go to zero as the chamber isn't a perfect conductor, and the modes appear to have several "beating" components forming shoulders, and other frequencies present, one of which is discussed below.

III. Gas Sample Spectrum

CSR operation typically requires two consecutive 8 hour shifts to allow for setup, long injection times and short beam lifetimes, ~ 4 hours, for taking data. This allows 4 minute scans to be taken over several hours. The noise level in a scan was large at higher beam currents, but dropped off with current decay. Preliminary CSR results in the 5 to 40 cm^{-1} region, led to measuring a gas phase sample, nitrous oxide N_2O. Figure 4 shows a 0.025 cm^{-1} resolution spectrum of 46 scans co-added. The high frequency structure is seen throughout.

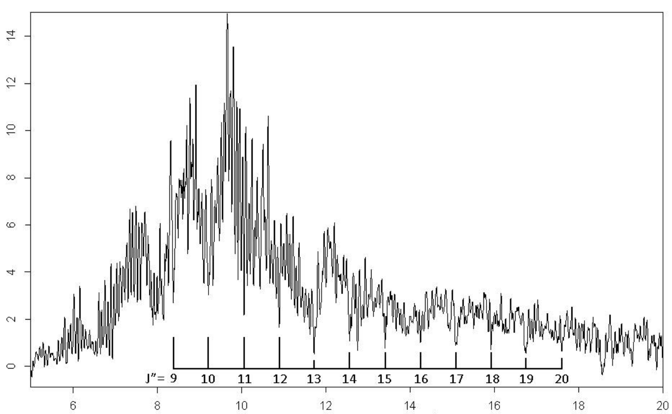

Figure 4: Spectrum of N_2O taken with CSR. Absorption lines are indicated for J" rotational transitions.

The curve shows pure rotational transitions within the ground vibrational state of N_2O. The J" numbers refer to the transition in rotation. J" means the lower level rotational quantum number, these transitions occur within the same level and are R-branch absorptions, so the change in J is +1. These absorption lines have an intrinsic width of ~2×10^{-5} cm^{-1} with the line at 15.918 cm^{-1} being measured at 0.0244 cm^{-1}. Data was taken with a 0.3 m multi-pass gas cell of 6 m pathlength, pressure of 1 Torr at 25 °C.

A coarse envelope structure of ~1 cm^{-1} spacing is discernible over the wider region that can be fitted with the same impedance model using a wall distance set to a nominal location (d = 49 mm) coinciding with the outer radius of the standard dipole chambers. The two IR chambers do not have the constriction so the outer wall is not constrained by the narrowing of the vacuum plenum. This implies that the bunch may have some "memory" of the impedance of the preceding chamber(s), via an unknown mechanism within the bunch distribution, that affects its emission in the IR chamber.

With a new ring configuration, and recent testing of single bunch fills, both faster injections and longer lifetimes are possible and will allow more scan time to examine operation in single and multi-bunch modes. As 0.001 cm^{-1} resolution scans can take 20 to 40 minutes per scan, this will enable practical experimental time for large numbers of scans. The fine structure in the energy curve will affect the spectroscopy to be performed in this region. Over a sufficiently small region gas samples may have several absorption peaks within a modal lobe and be amenable to analysis. However, hundreds of transitions typically span many wavenumbers, and the sensitivity across many modes will vary considerably, complicating analysis. If the fine structure is stable, ratioing sample to background will remove the baseline fluctuation, but the variance in S/N may be problematic for sensitive work. The suitability of burst mode CSR for ultra high resolution gas phase may be limited in this regard.

References

[1] See http://infrared.als.lbl.gov/content/web-links/45-srir or http:// www.lightsources.org,

[2] Y.-L. Mathis, B. Gasharova and D. Moss, "Terahertz Radiation at ANKA, the New Synchrotron Light Source in Karlsruhe," J. Biol. Physics vol. 29, 2003, pp. 313–318.

[3] P. Roy, et.al., "The AILES Infrared Beamline on the third generation Synchrotron Radiation Facility SOLEIL," Infrared Phys. & Tech. vol. 49, no.1-2, 2006, pp. 139-146.

[4] D. Creagh, J. McKinlay and P. Dumas, "The design of the infrared beamline at the Australian synchrotron," Vibr. Spectroscopy, vol. 41, no. 2, 2006, pp. 213-220.

[5] T. E. May, R. A. Bosch , et.al., "“Infrared edge radiation beamline at Aladdin,” Proc. Particle Acceleration Conference, 1999, pp. 2394-6.

[6] U. Arp, G.T. Fraser, et.al., "Spontaneous coherent microwave emission and the sawtooth instability in a compact storage ring," Phys. Rev. Special Topics vol. 4, 2001, pp. 054401-1,9.

[7] A. Andersson, M. S. Johnson, B. Nelander, "Coherent synchrotron radiation in the far infrared form a 1-mm electron bunch," Opt. Eng. vol. 39, no. 12, pp. 3099-105.

[8] M. Abo-Bakr, K Feikes, et.al., "Steady-state Far-Infrared Coherent Synchrotron Radiation detected at BESSY II," Phys. Rev. Let. vol. 88, no. 25, pp. 254801-1,4.

[9] J. M. Byrd, W. P. Leemans, et.al., "Observation of Broadband Self-Amplified Spontaneous Coherent Terahertz Synchrotron Radiation in a Storage Ring," Phys. Rev. Let., vol. 89, no. 22., 2002, pp. 224801-1,4.

[10] G. L. Carr, S. L. Kramer, et.al., "Observation of coherent synchrotron radiation from the NSLS VUV ring," NIMA v. 463, 2001, pp. 387-392.

[11] F. Sannibale, et.al., "A model describing stable coherent synchrotron radiation in storage rings," Phys. Rev. Let. vol. 93, no. 9, 2004, pp. 094801-1,4.

[12] T. E. May, D. A. Appadoo, et.al., "Infrared beamlines at the Canadian Light Source," 9th Intl. S.R.I. AIP Conf. Proc. 879 2006, pp. 579-582.

[13] T. May, D. Appadoo, "Far Infrared Beamline 02B1-1," Canadian Light Source Activity Report 2007, pp.151-2.

[14] M. Abo-Bakr et.al., “Brilliant, Coherent Far-Infrared (THz) Synchrotron Radiation,” Phys. Rev. Let., vol. 90, no.9, 2003, pp. 094801-1,4.

[15] R. L. Warnock and P. Morton, “Fields Excited by a Beam in a Smooth Toroidal Chamber. Part 1:Longitudinal Coupling Impedance.”, Particle Accelerators, vol. 25, 1990, pp. 113-184.

[16] U. Schade, et.al., "New Infrared spectroscopic beamline at BESSY II," Rev. Sci. Instr. vol. 73, no. 3, 2002, pp.1568-1570.

[17] J. M. Byrd, W. P. Leemans, et.al., "Observation of Broadband Self-Amplified Spontaneous Coherent Terahertz Synchrotron Radiation in a Storage Ring," Phys. Rev. Let., vol. 89, no. 22., 2002, pp. 224801-1-